



# Carboxymethylation of viscose and cotton fibers: comparisons of water retention and moisture sorption

Paul Bogner · Inge Schlapp-Hackl ·  
Michael Hummel · Thomas Bechtold ·  
Tung Pham · Avinash P. Manian

Received: 31 May 2024 / Accepted: 24 August 2024  
© The Author(s) 2024

**Abstract** The aim of the work was to compare the water retention and moisture sorption of viscose (CV) and cotton (Co) fibers carboxymethylated from aqueous media, in presence of NaOH, with sodium monochloroacetate. It was shown previously that under the same treatment conditions, the degree of carboxymethylation was higher in CV and so was the depth within fiber structures to which the carboxymethylation reactions occurred. It was also shown previously, that in terms of their capacity for sorption of a cationic dye (methylene blue), the Co performed better than CV. In this work, the same fibers were tested for their water retention and moisture sorption propensities. The two were sensitive both to the degree of carboxymethylation *and* the inherent properties of fibers (accessibility, degree of swelling, hornification). But the moisture sorption levels were less sensitive to the degree of carboxymethylation and more to inherent

fiber properties whereas the reverse was observed for water retention. In contrast to the prior observations with dye sorption, CV performed better than Co in both moisture sorption and water retention. The poor performance of CV in dye sorption was attributed to the greater depth of carboxymethylation within the fibers that hindered dye permeation, but the same feature was observed to result in better performance (water retention) or not to hinder performance (moisture sorption). These observations highlight the contrasting effects that may arise, of a given set of treatment parameters (fiber type, alkali level in treatment), on efficacy of the product performance.

**Keywords** Cellulose · Cotton · Viscose · Carboxymethylation · Water retention · Moisture sorption

---

**Supplementary Information** The online version contains supplementary material available at <https://doi.org/10.1007/s10570-024-06144-9>.

---

P. Bogner · T. Bechtold · T. Pham · A. P. Manian (✉)  
Research Institute of Textile Chemistry/Physics,  
Universität Innsbruck, Hoehsterstrasse 73,  
6850 Dornbirn, Austria  
e-mail: avinash.manian@uibk.ac.at

I. Schlapp-Hackl · M. Hummel  
Department of Bioproducts and Biosystems, School  
of Chemical Engineering, Aalto University, P.O.  
Box 16300, 0076 Aalto, Finland

## Introduction

The carboxymethylation of cellulose is of interest for use in applications such as products for water or moisture sorption (Miyamoto et al. 2018; Chen et al. 2022), or in the removal of contaminants from wastewater (Yan et al. 2011; Wang et al. 2019, 2023). The carboxymethyl derivative of cellulose is obtained through a Williamson-type etherification of a hydroxyl group, in presence of alkali, through nucleophilic substitution with monochloroacetic acid (Mischnick and Momcilovic 2010). To create robust

structures capable of withstanding the mechanical stresses generated in such applications, the carboxymethyl cellulose may be deposited and fixed on a carrier (Ibrahim et al. 2020), fibers may be spun from dopes containing carboxymethyl cellulose for assembly into networks (Wang et al. 2023), or cellulose fibers may first be assembled into networks and then subjected to the derivatization reaction (Rác et al. 1995). The latter route is of interest for sectors such as textiles and nonwovens, where large-scale chemical treatments of fibrous assemblies are a routine part of operations. However, one limitation in the textiles and nonwovens sectors is the strong preference for water as solvent, as most chemical treatment operations are performed in open-to-air vessels. Thus, although optimal reaction yields in carboxymethylation of cellulose is known to be achieved in alcohol-rich media (Gu et al. 2012; Heinze et al. 2018; Li et al. 2022; Liao et al. 2022; Liu et al. 2023; Thakur et al. 2023), aqueous media-based carboxymethylation is preferred in textile treatments.

The carboxymethylation from aqueous media proceeds in a heterogeneous mode, i.e., the reactions occur from liquid media on solid fibrous substrates. In such conditions, the availability of accessible sites (or accessibility) becomes important in governing the progress in reactions, i.e., how much of the fibrous substrate is derivatized and how the introduced functional groups are distributed through the fiber bulk. The source of cellulose acquires importance, as both native and regenerated cellulosic fibers may be employed in the creation of fibrous networks, and they differ in morphological features (e.g., total porosity and the distribution of pores through their structures) as well as supramolecular structure (e.g., degrees of polymerization and of crystallinity)—and both may act to determine the accessibility in fibers. Also of interest is performance, i.e., will celluloses from different sources, with the same overall degree of carboxymethylation, perform to the same level in a given test, e.g., of dye or water sorption.

In previous communications (Bogner et al. 2024a, b), we reported on the carboxymethylation of viscose (CV) and cotton (Co) fibers—a regenerated and native cellulosic respectively—from aqueous solutions of sodium monochloroacetate and NaOH. The treatment parameters were varied: NaOH level in reaction media (0.5 M and 4.0 M), temperature (30 °C and 50 °C) and the content of sodium monochloroacetate, to obtain

CV and Co fibers with a range of carboxymethyl group contents. It was determined that under comparable treatment conditions, the degree of carboxymethylation was greater in CV as compared to Co, and also that the depths in fibers to which carboxymethylation occurred, was higher in CV as compared to Co. When the fibers were tested for performance in terms of their capability for sorption of a cationic dye (methylene blue), the molar ratio of dye sorption to carboxyl groups on fibers was higher in Co as compared to CV. The differences were attributed to greater restrictions on permeation of the dye through the CV as compared to Co fibers. In this communication, we report on measurements of the performance of the derivatized CV and Co fibers in their capacity for interactions with liquid water (measured through water retention) and water vapor (measured through moisture sorption). The results of measuring the degree of crystallinity in fibers and of their degrees of polymerization are also reported.

## Materials

The viscose (CV) fibers were donated by Kelheim Fibres GmbH (Germany) and the cotton (Co) was donated by Gebr. Otto Baumwollfeinzwirnerei GmbH+Co. KG (Dietsheim, Germany). The procedures for their cleaning, their carboxymethylation treatments and the resulting degrees of carboxymethylation are all reported previously (Bogner et al. 2024a, b).

In brief, CV and Co fibers were cleaned, and awarded carboxymethylation treatments from aqueous reaction media containing sodium monochloroacetate and NaOH. The alkali content in reaction media was maintained at either 0.5 M or 4.0 M, and the treatment temperature at 30 °C or 50 °C. Fibers that were only cleaned and treated only with 4.0 M NaOH were employed as reference. The carboxymethylation degree was estimated from sample carboxyl contents. The values, as determined with potentiometric titration, are summarized in Table 1.

## Methods

Fourier transform infrared (FTIR) spectroscopy

FTIR spectroscopy, with measurements both in Attenuated Total Reflectance (ATR) mode and

**Table 1** Range of carboxyl contents (mmol COOH/kg) observed in Co and CV fibers from the different treatment sets. From previous work (Bogner et al. 2024a, b)

Treatment	Co	CV
Only cleaned	18.7	67.5
Treated only with 4.0 M NaOH	19.1	63.7
Reactions in 0.5 M NaOH (30 °C and 50 °C)	54.8–173.7	169.6–377.3
Reactions in 4.0 M NaOH (30 °C and 50 °C)	65.1–436.8	168.9–545.4

transmittance mode (KBr pelleting), was previously utilized to assess the uniformity of carboxymethyl group distribution through fiber structures (Bogner et al. 2024a, b). The same spectra are utilized here to assess changes in crystallinity of fibers as a result of treatments.

### Gel permeation chromatography (GPC)

The average molecular weight and molar mass distribution in selected samples was determined with gel permeation chromatography (GPC), following a method described previously (Pitkänen and Sixta 2020; Rissanen et al. 2023). The device was a Dionex Ultimate 3000 HPLC Module (Thermo Fisher Scientific Inc., Waltham USA) equipped with a Shodex DRI (RI-101) detector (Showa Denko, Ogimachi, Japan) and a Viscotek/Malvern SEC/MALS 20 multi-angle light scattering (MALS) detector (Malvern Panalytical Ltd., Malvern, UK). The fiber specimens ( $50 \pm 5$  mg) were activated through sequential immersion in water, acetone, and dimethylacetamide (DMAc), before being dissolved in 5 ml of a 90 g/L LiCl/DMAc (saturated solution) and diluted to a concentration of 1.0 mg/ml with pure DMAc. The analyses were performed in ambient temperature by injecting 100  $\mu$ l volumes at a flow rate of 0.75 ml/min through a set of four PLgel MIXED-A columns (Agilent Technologies Inc., Palo Alto, USA).

The DRI and MALS detector constants were established and tested with polystyrene standards dissolved in 90 g/L LiCl/DMAc. The polystyrene standards were obtained from Polymer Standards Service (Mainz, Germany): one with narrow molecular weight distribution ( $M_w = 96,000$  g/mol,  $D = 1.04$ , refractive index increment,  $\partial n/\partial c$ , 0.146 ml/g) and one with broad molecular weight distribution ( $M_w = 248,000$  g/mol,  $D = 1.73$ ). The standards employed for calibration were cello-oligosaccharides (cellobiose, cellotriase, cellotetraose, cellopentaose) and linear xylo-oligosaccharides (xylobiose,

xylotriase, xylo-tetraose) purchased from Megazyme Ltd. (Wicklow, Ireland). A  $\partial n/\partial c$  value of 0.136 ml/g measured at 488 nm was used for the cellulose dissolved in 90 g/L LiCl/DMAc.

### Protonation/deprotonation

The moisture sorption and water retention measurements described below were performed both on protonated and deprotonated specimens. For that, specimens were immersed for 1 h at ambient temperature in solutions of 0.1 M HCl (protonation) or 0.1 M NaOH (deprotonation), and then rinsed repeatedly with deionized water until the pH of the rinse water was similar to that of fresh deionized water. The wet specimens after the last rinsing step were used directly for measurements of water retention, but the specimens were allowed to dry in ambient atmosphere prior to measurements of moisture sorption.

### Intrinsic viscosity determination

According to SCAN-CM 15:88, the standard for Scandinavian pulp, paper, and board testing, the intrinsic viscosities,  $\eta$  (ml/g), of the materials were evaluated. Thereby the viscosity was determined in a cupri-ethylenediamine solution via a capillary-tube viscometer. The Mark-Houwink equation was used to calculate the degree of polymerization (DP).

### Moisture sorption/desorption

The moisture sorption and desorption equilibria and kinetics over the humidity range 0–90% at 25 °C, was measured on an automated multi-sample Dynamic Vapor Sorption analyzer (V sorp, proUmid GmbH & Co. KG, Ulm, Germany). About 100 mg specimens were placed in aluminum dishes and loaded onto the device, where the atmosphere was initially conditioned to 0% relative humidity. The specimen masses were recorded every 10 min until attainment

of equilibrium (defined as mass change of less than 0.05% over 300 min), whereupon the relative humidity was raised to the next level. This procedure was repeated as relative humidity levels were raised stepwise from 0% through 10%, 20%, 30%, 40%, 50%, 60%, 70%, 80%, 90% (sorption phase of measurement) and lowered in the reverse order (desorption phase of measurement). The moisture level in specimens at any given point was quantified in terms of the moisture regain (MR), calculated as shown in Eq. 1:

$$MR = \frac{m_x - m_0}{m_0} \times 100 \quad (1)$$

where, MR=moisture regain (%),  $m_x$ =mass of specimen (g) at given point,  $m_0$ =equilibrium mass of specimen (g) at 0% relative humidity.

The fitting of kinetic and equilibrium sorption models to experimental data was achieved by non-linear regression with the software SigmaPlot (version 14.0, Systat Software GmbH, Germany).

#### Water retention

About 0.1 g fiber specimens, after protonation/deprotonation and rinsing, were transferred to filtration tubes of 0.45  $\mu\text{m}$  porosity, centrifuged for 10 min at  $4000 \times g$ , weighed, dried in ambient atmosphere and reweighed. The water retention values (WRV) were calculated with Eq. 2.

$$WRV = \frac{m_{wet} - m_{dry}}{m_{dry}} \times 100 \quad (2)$$

where, WRV=water retention value (%),  $m_{wet}$ =mass of wet fiber after centrifugation (g),  $m_{dry}$ =mass of fiber after drying in ambient atmosphere (g).

## Results and discussion

#### FTIR spectroscopy

Typical FTIR spectra of CV and Co fibers, from reference treatments (i.e., only cleaned, and treated with 4.0 M NaOH alone) and carboxymethylation treatments (in 0.5 M NaOH and 4.0 M NaOH), from both ATR and transmission mode of measurements, are shown in Fig. S1, along with assignments for the absorbance peaks discussed below.

Cellulose swells in aqueous solutions of NaOH, with a transition observed at ca. 4.0 M, from intercrystalline to intracrystalline swelling (Klemm et al. 1998a). Both inter- and intracrystalline swelling may lead to porosity and therefore accessibility changes. Intracrystalline swelling leads also to an irreversible transformation in the crystal structure of native celluloses (e.g., Co) from polymorph type I to type II (O'Sullivan 1997). That can be detected in FTIR spectra, as demonstrated previously (Manian et al. 2022), from changes in peak intensity, shape or position at the wavenumber regions of 3484–3488  $\text{cm}^{-1}$ , 3410–3450  $\text{cm}^{-1}$ , 3300–3340  $\text{cm}^{-1}$ , 3270  $\text{cm}^{-1}$ , 1429  $\text{cm}^{-1}$ , 1163  $\text{cm}^{-1}$ , 1111  $\text{cm}^{-1}$  and 893  $\text{cm}^{-1}$ . Regenerated celluloses (e.g., CV) originally exhibit polymorph type II in their crystalline domains, which is thermodynamically the most stable among all cellulosic polymorphs, and thus intracrystalline swelling does not change the polymorph type.

The Co fibers subjected only to cleaning or to carboxymethylation treatments in 0.5 M NaOH (at either 30 °C or 50 °C), all exhibited evidence of polymorph type I in their spectra; while those treated in 4.0 M NaOH alone, or carboxymethylated in 4.0 M NaOH (at 30 °C or 50 °C), showed evidence of polymorph type II. This was observed in both ATR mode (representative of the fiber surface) and transmission mode (representative of the fiber bulk). It shows that under the treatment conditions employed in experiments, there was thorough impregnation of NaOH solutions through the fiber structures. All CV fibers exhibited evidence of the polymorph type II in their spectra.

The spectra may also be utilized to evaluate indices of crystallinity in the fibers, from the ratios of absorbance intensities at wavenumber regions of 1376  $\text{cm}^{-1}$ /2902  $\text{cm}^{-1}$  ("Total Crystallinity Index, TCI") (Nelson and O'Connor 1964), 1420  $\text{cm}^{-1}$ /893  $\text{cm}^{-1}$  ("Lateral Order Index, LOI") (O'Connor et al. 1958) and 3366  $\text{cm}^{-1}$ /1336  $\text{cm}^{-1}$  ("Hydrogen Bond Intensity, HBI") (Nada et al. 2000). The TCI and LOI are directly proportional, and the HBI is inversely proportional, to the degree of crystallinity (Oh et al. 2005a, b). The indices from FTIR spectroscopy have been shown to correlate with degrees of crystallinity derived from X-ray Diffraction (XRD) (Nelson and O'Connor 1964). The proportionality of LOI with XRD results for polymorph type I is not the same as with polymorph type II, but

the proportionalities of TCI and HBI do not vary with polymorph type.

The FTIR crystallinity indices of the CV and Co fibers, from both the ATR and transmission modes of measurements, are shown in Fig. S2. The TCI and LOI from transmission mode measurements were greater than those from the ATR mode, while the converse was observed for the HBI. That suggests differences in crystallinity between the fiber bulk and their surfaces. Only marginal and inconsistent differences could be discerned in the indices as function of fiber type (Co vs. CV), treatment type (i.e., NaOH content in treatment), or the degree of carboxymethylation. The exception was the consistent differences in LOI between the type I polymorph (i.e., Co not treated with 4.0 M NaOH) and type II polymorph (i.e., Co treated with 4.0 M NaOH and all CV fibers). That may be attributed to the difference between the polymorph types in proportionality of the LOI with degree of crystallinity.

#### Intrinsic viscosities, DP and molar mass distribution

The degree of polymerization (DP) was calculated from the intrinsic viscosity values determined by dissolving the samples in a cupri-ethylenediamine solution according to a common procedure (SCAN-CM 15:88). The commonly reported procedures for determination of molecular weight and molecular weight

distribution of carboxymethyl cellulose with GPC involve dissolution of the polymer in eluent made of water alone or water containing NaOH, CH<sub>3</sub>COOH/CH<sub>3</sub>COONa, NaCl, Na<sub>2</sub>SO<sub>4</sub>, NaNO<sub>3</sub> or NaNO<sub>3</sub>/NaH<sub>2</sub>PO<sub>4</sub> (Eremeeva and Bykova 1998; Wach et al. 2003; Cleaver 2015a, b; Iwata 2021; Kunjalukkal Padmanabhan et al. 2023). The minimum degree of substitution required for water solubility of carboxymethyl cellulose is about 0.4 (BeMiller 2019), but the degree of substitution measured in this work ranged between 0.01–0.07 (Co) and 0.01–0.09 (CV) (Bogner et al. 2024a, b). Thus, the eluent employed for GPC measurements was that commonly used for cellulose (LiCl/DMAc). The chromatograms are shown in Fig. S3 and the derived parameters are listed in Table 2.

The chromatograms of most carboxymethylated samples (marked with an asterisk in Table 1) showed signs of molecular aggregation in eluent (see Fig. S3), in that larger weight fractions were observed in the higher molecular weight region, as compared to the reference (i.e., only cleaned fibers). One possible reason may be presence of moisture, as that has been shown to induce molecular aggregation between polymer chains in solutions of cellulose in LiCl/DMAc (Potthast et al. 2002; Röder et al. 2002). It is also possible that the chosen eluent system was not suitable for the carboxymethylated samples despite the relatively low degrees of substitution. Thus,

**Table 2** Results from measurements of intrinsic viscosities (ml/g), DP, number average molar masses Mn (kDa), weight average molar masses Mw (kDa), poly dispersity indices (PDI, Mw/Mn) on selected samples

Fiber	Treatment	COOH <sup>a</sup> (mmol/kg)	$\eta^b$ (ml/g)	DP <sub><math>\eta</math></sub> <sup>c</sup>	Mn (kDa)	Mw (kDa)	Mw/Mn
CV	Cleaned	67	156 ± 3	372	19.4 ± 0.7	42.1 ± 0.5	2.2 ± 0.1
	0.5/50 <sup>d,*</sup>	377	147 ± 3	350	22.7 ± 0.5	77.3 ± 0.9	3.4 ± 0.1
	4.0/30*	545	153 ± 8	364	34.5 ± 2.5	102.6 ± 9.5	3.0 ± 0.1
	4.0/30	318	161 ± 1	383	19.4 ± 1.5	35.4 ± 2.2	1.8 ± 0.1
Co	Cleaned	19	556 ± 4	1385	95.9 ± 5.1	177.4 ± 3.5	1.9 ± 0.1
	0.5/50*	111	492 ± 2	1180	51.3 ± 9.3	125.6 ± 7.2	2.5 ± 0.3
	4.0/30*	437	474 ± 7	1124	99.3 ± 8.6	240.8 ± 17.1	2.4 ± 0.1
	4.0/30*	135	487 ± 10	1164	109.5 ± 2.7	245.1 ± 1.3	2.2 ± 0.1

\*denotes samples showing signs of molecular aggregation in their chromatograms

<sup>a</sup>carboxyl content,

<sup>b</sup>average intrinsic viscosity,

<sup>c</sup>degree of polymerization derived from the average intrinsic viscosity,

<sup>d</sup>denotes the NaOH content (M)/temperature (°C) during carboxymethylation treatment

more work will be required towards optimization of the measurement methodology in future, in terms of either the sample preparation regime and/or choice of eluent. Nevertheless, the viscometry results showed that the degree of polymerization was greater in Co as compared to CV (which was expected) and that the carboxymethylation treatments reduced the degree of polymerization on average by about 10% in CV and about 15% in Co fibers. It shows no significant oxidative damage during treatments, which is also supported by the fact there were no significant changes in fiber carboxyl content after treatments with alkali alone (see Table 1).

#### Water retention (WRV)

The WRV of the protonated and deprotonated forms of fibers are plotted against their carboxyl contents in Fig. 1. In both sets (i.e., protonated and deprotonated), the WRV increased in the order of fiber type/NaOH level: Co/0.5 M < Co/4.0 M  $\cong$  CV/0.5 M < CV/4.0 M. In other words, at comparable levels of carboxymethylation, the WRV was higher in CV as compared to Co, and in fibers from 4.0 M NaOH treatments as compared to 0.5 M NaOH treatments. And, the WRV of Co from the 4.0 M NaOH treatments and CV from the 0.5 M NaOH treatments, were similar.

The effect of carboxymethylation degree on WRV was found to be greater in the deprotonated as compared to protonated fibers. In the protonated set, the WRV did not change with increase in carboxyl content among fibers from the 0.5 M NaOH treatments; and among fibers from the 4.0 M NaOH treatments, a gradual rise in WRV was observed, with both CV and Co exhibiting similar gradients. In the deprotonated set, the WRV increased with rise in carboxyl content in all fibers, with the gradients increasing in the following order of fiber type/NaOH level: Co/0.5 M  $\cong$  CV/0.5 M < Co/4.0 M < CV/4.0 M; i.e., the gradient was higher in fibers from the 4.0 M NaOH as compared to 0.5 M NaOH treatments, and in CV as compared to Co.

The WRV of deprotonated forms of fibers was higher than that of the protonated forms, and the proportion varied only with the degree of carboxymethylation. The ratio of WRVs, deprotonated-to-protonated, increased from about 1 (observed in the reference fibers), in near-linear fashion, to about 2 in fibers with the highest degree of carboxymethylation in the experimental set, with no differences being apparent as function of either the fiber type or the NaOH level.

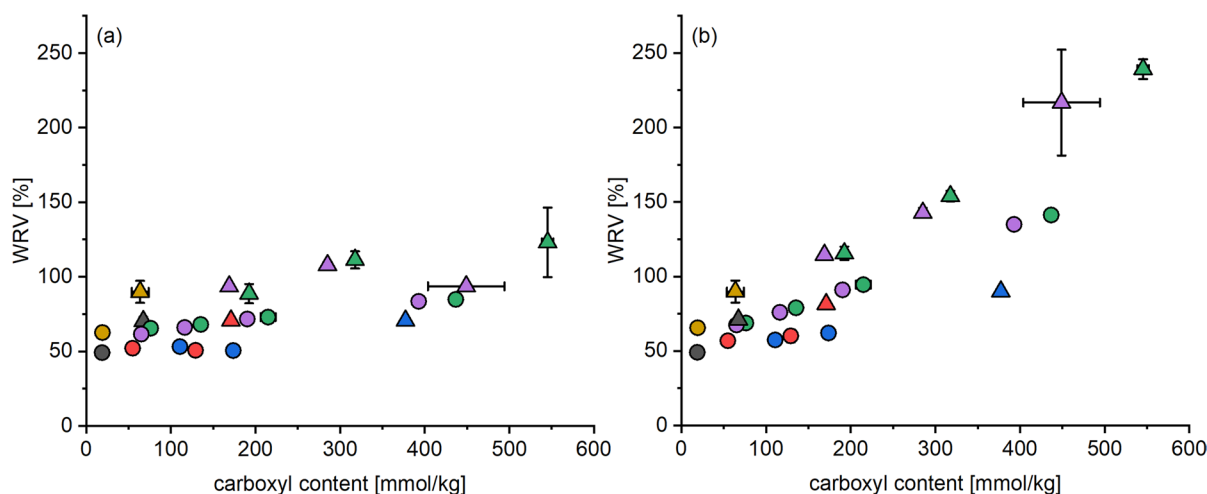


**Fig. 1** The WRV of **a** protonated and **b** deprotonated forms of the fibers. The circles are data from Co fibers, and the triangles from CV fibers. The marker colors represent treatment sets: cleaned fibers (black circle, black triangle), fibers treated only in 4.0 mol/L NaOH (yellow circle, yellow trian-

gle), in 0.5 mol/L NaOH at 30 °C (red circle, red triangle), in 0.5 mol/L NaOH at 50 °C (blue circle, blue triangle), in 4.0 mol/L NaOH at 30 °C (green circle, green triangle) and in 4.0 mol/L NaOH at 50 °C (violet circle, violet triangle)

## Moisture sorption isotherms

The moisture sorption isotherms measured on all fibers, both protonated and deprotonated forms, exhibited the characteristics of a Type II isotherm in the IUPAC classification (Thommes et al. 2015), which is typical for moisture sorption on cellulose. Selected examples from the deprotonated set are shown in Fig. 2. A hysteresis was observed, i.e., at equivalent humidity levels, the moisture regain equilibria from the desorption phase were greater than that from the sorption phase. The aggregate hysteresis was calculated with Eq. 3, and the values are shown in Fig. S4.

$$\sum H = \frac{\sum MR\%_{Desorp} - \sum MR\%_{Sorp}}{\sum MR\%_{Sorp}} \quad (3)$$

where,  $\sum H$  = aggregate hysteresis,  $\sum MR\%_{Desorp}$  = sum of moisture regain equilibria in the range 10–80% of relative humidity from the desorption phase of measurement,  $\sum MR\%_{Sorp}$  = sum of moisture regain equilibria in the range 10–80% of relative humidity from the sorption phase of measurement.

Generally, no significant differences were observed in aggregate hysteresis levels between the protonated and deprotonated forms of fibers or as

function of fiber type, the NaOH level and degree of carboxymethylation.

## Moisture regain equilibria (sorption phase)

The equilibria at each of the relative humidity levels (10–90%), as function of the degree of carboxymethylation and NaOH level during treatment, on both the protonated and deprotonated forms of fibers, are shown in Fig. 3 and 4 respectively.

At each humidity level, at comparable levels of carboxymethylation, moisture regain equilibria generally increased in the order of fiber type/NaOH level: Co/0.5 M < Co/4 M < CV/0.5 M  $\cong$  CV/4 M. In other words, the highest moisture regain was observed in CV, with no significant differences between fibers from 4.0 M NaOH or 0.5 M NaOH treatments. The moisture regain in Co was lower, and fibers treated in 4.0 M NaOH exhibited greater moisture regain than fibers treated in 0.5 M NaOH. This was observed for both the protonated and deprotonated forms of fibers.

The sensitivity of moisture regain equilibria to degree of carboxymethylation was greater in Co as compared to CV. The protonated forms of CV exhibited almost no change in moisture sorption with rise in carboxymethylation degree, but in their

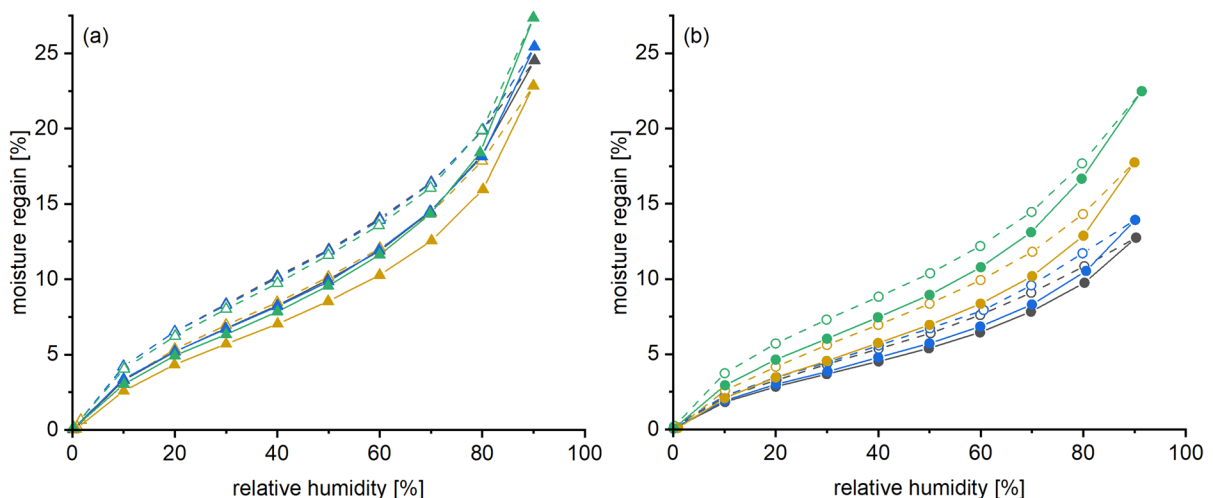


**Fig. 2** Selected examples of moisture sorption isotherms from **a** CV and **b** Co fibers. Results from the deprotonated forms of fibers are shown. The marker colors represent treatment sets: cleaned fibers (black circle, black triangle), fibers treated only in 4.0 mol/L NaOH (yellow circle, yellow triangle), in 0.5 mol/L NaOH at 50 °C (blue circle, blue triangle),

in 4.0 mol/L NaOH at 30 °C (green circle, green triangle). The circles are data from Co fibers, and the triangles from CV fibers. Solid markers connected by solid lines represent data from the sorption phase and the hollow markers connected by dashed lines represent data from the desorption phase of experiments

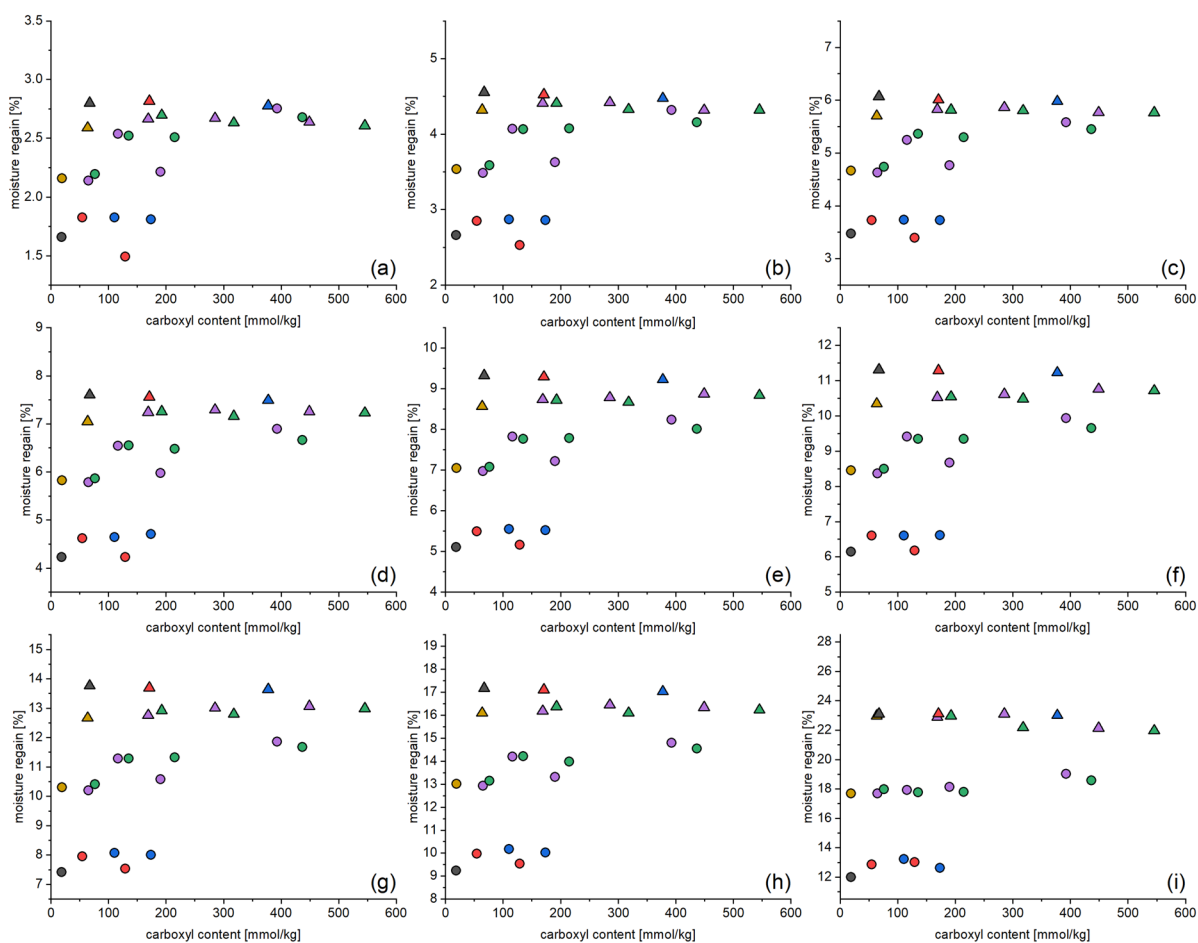


**Fig. 3** Moisture regain equilibria as function of carboxyl content, measured in the sorption phase of experiments, on the protonated forms of fibers, at each of the relative humidity levels **a** 10%, **b** 20%, **c** 30%, **d** 40%, **e** 50%, **f** 60%, **g** 70%, **h** 80%, **i** 90%. The circles are data from Co fibers, and the triangles from CV fibers. The marker colors represent treat-

ment sets: cleaned fibers (black circle, black triangle), fibers treated only in 4.0 mol/L NaOH (yellow circle, yellow triangle), in 0.5 mol/L NaOH at 30 °C (red circle, red triangle), in 0.5 mol/L NaOH at 50 °C (blue circle, blue triangle), in 4.0 mol/L NaOH at 30 °C (green circle, green triangle) and in 4.0 mol/L NaOH at 50 °C (violet circle, violet triangle)

deprotonated form, there was a gradual rise in moisture regain with increase in carboxymethylation degree. The change in moisture regain of Co with rise in carboxymethylation degree was higher. The gradients were higher in the deprotonated as compared to protonated forms, and in fibers from the 4.0 M NaOH as compared to 0.5 M NaOH treatments.

The moisture regain equilibria of deprotonated forms was greater than the corresponding protonated forms, and the proportions varied with the degree of carboxymethylation and relative humidity. The ratios, deprotonated-to-protonated, were

always in the region of 1 for the reference fibers at all humidity levels. For fibers with the highest degree of carboxymethylation, the ratios were in the region of 1.07 at 10% relative humidity, between 1.08–1.10 in the relative humidity interval 20–60%, and increased from about 1.11–1.20 as the relative humidity increased from 70 to 90%. At each humidity level, the ratios changed in near-linear fashion with degree of carboxymethylation. No significant influence appeared of either fiber type or NaOH level.



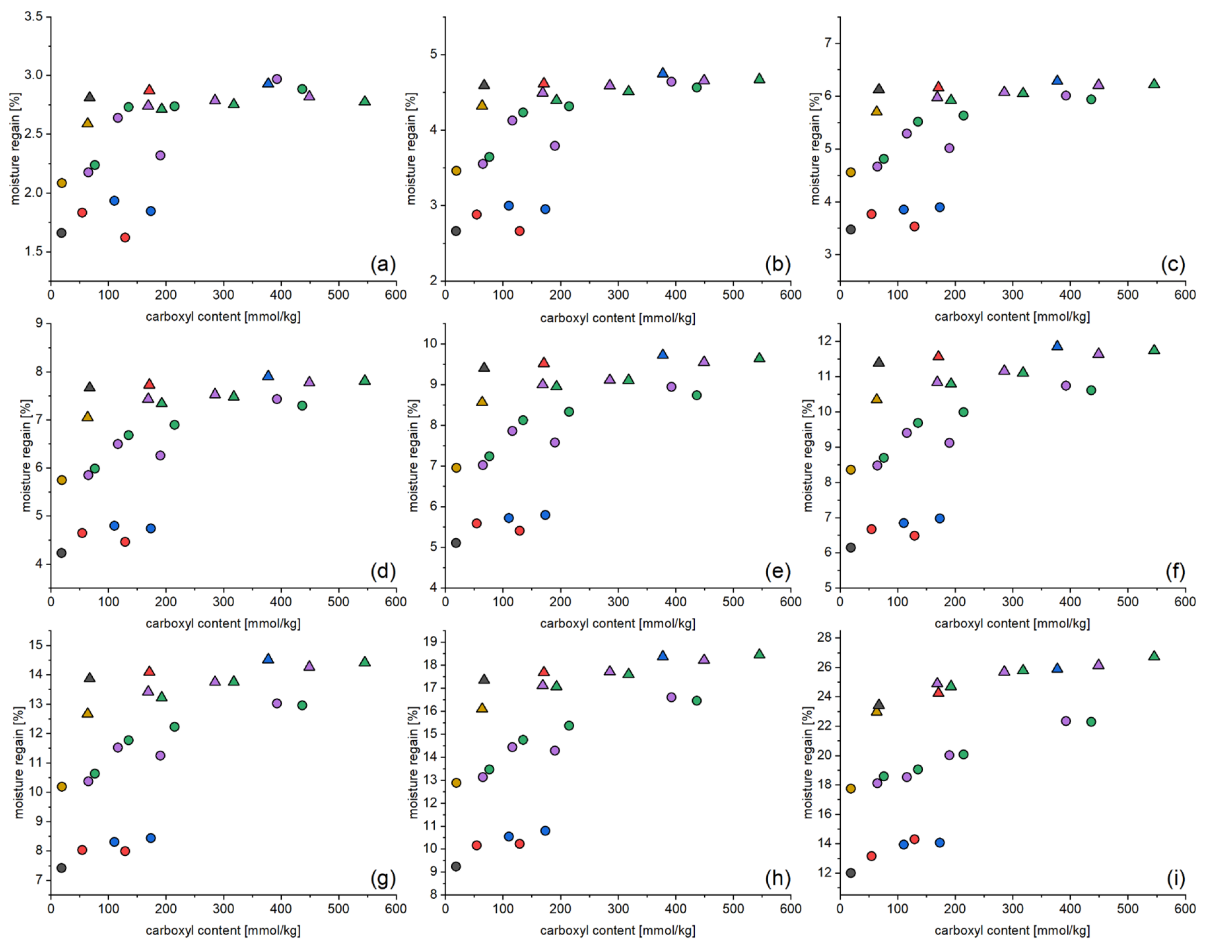


**Fig. 4** Moisture regain equilibria as function of carboxyl content, measured in the sorption phase of experiments, on the deprotonated forms of fibers, at each of the relative humidity levels **a** 10%, **b** 20%, **c** 30%, **d** 40%, **e** 50%, **f** 60%, **g** 70%, **h** 80%, **i** 90%. The circles are data from Co fibers, and the triangles from CV fibers. The marker colors represent treat-

ment sets: cleaned fibers (black circle, black triangle), fibers treated only in 4.0 mol/L NaOH (yellow circle, yellow triangle), in 0.5 mol/L NaOH at 30 °C (red circle, red triangle), in 0.5 mol/L NaOH at 50 °C (blue circle, blue triangle), in 4.0 mol/L NaOH at 30 °C (green circle, green triangle) and in 4.0 mol/L NaOH at 50 °C (violet circle, violet triangle)

### Guggenheim-Anderson-de Boer (GAB) model

The Type II isotherms observed in the sorption phase of moisture sorption/desorption measurements were characterized with the GAB model, shown in Eq. 4.

$$v = \frac{v_m \cdot C \cdot k \cdot \frac{p}{p^0}}{\left(1 - k \cdot \frac{p}{p^0}\right) \cdot \left\{1 + (C - 1) \cdot k \cdot \frac{p}{p^0}\right\}} \quad (4)$$

where,  $v$  = equilibrium moisture regain (g/g),  $v_m$  = moisture sorbed as a monomolecular layer (g/g),  $C$  = energy constant, proportional to the

difference in free enthalpy of water between its pure liquid state and in the monolayer,  $k$  = average measure of the difference in free enthalpy of water between its pure liquid state and in the sorbed layers beyond the first (i.e., monolayer),  $p/p^0$  = relative humidity expressed as partial pressure.

Like the Brunauer–Emmett–Teller (BET) model commonly used for Type II isotherms, the GAB model also describes multilayer sorption. While the BET is based on the assumption that adsorbate-sorbent interactions do not extend beyond the first sorbed layer (i.e., monomolecular layer), the GAB model is based on the principle that adsorbate-sorbent

interactions extend beyond the first sorbed layer and diminish progressively to zero over a finite distance (Timmermann 2003; Thommes et al. 2015). The thermodynamic state of sorbate molecules in that distance, differs from that of sorbate as pure liquid, by an average factor ‘ $k$ ’ ( $0 < k \leq 1$ ). The BET and GAB models are related, in that  $C_{\text{BET}} \equiv C_{\text{GAB}} \cdot k$ , and when  $k = 1$ , the GAB equation reduces to that of the BET. The advantage of GAB is the broader range of humidity available for model fitting (up to  $p/p^o = 0.8\text{--}0.9$ ) as compared to the BET (up to  $p/p^o = 0.3$ ).

The values of the parameter  $v_m$  are plotted in Fig. 5 for both CV and Co as function of the degree of carboxymethylation. At comparable degrees of carboxymethylation, the  $v_m$  increased in the order of fiber type / NaOH level: Co/0.5 M < Co/4.0 M  $\leq$  CV/4.0 M < CV 0.5 M. In other words, the  $v_m$  was generally greater in CV as compared to Co. In Co, the  $v_m$  was higher for fibers from the 4.0 M NaOH as compared to the 0.5 M NaOH treatments, but the reverse was observed in CV fibers. There was some overlap in  $v_m$  values between CV and Co from the 4.0 M NaOH treatments.

Changes to the  $v_m$  with rise in degree of carboxymethylation were higher in Co as compared to CV fibers, and higher in fibers from the 4.0 M NaOH treatments as compared to the 0.5 M NaOH treatments.

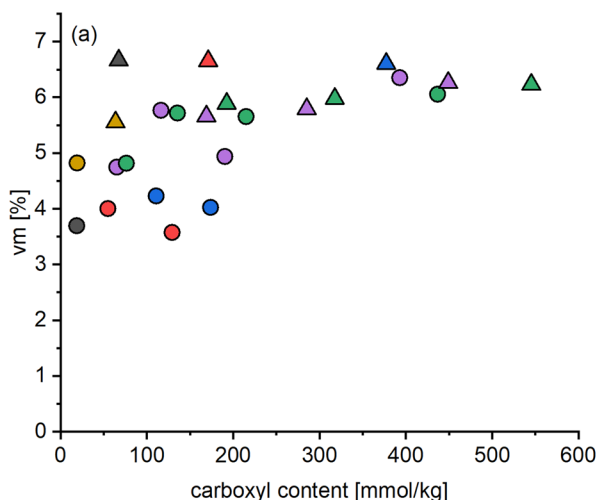


**Fig. 5** Values of the GAB model parameter  $v_m$  as function of carboxyl content, from measurements on **a** protonated and **b** deprotonated forms of fibers. The circles are data from Co fibers, and the triangles from CV fibers. The marker colors represent treatment sets: cleaned fibers (black circle, black triangle),

There were no significant differences of the  $v_m$  between the protonated and deprotonated forms of the fibers.

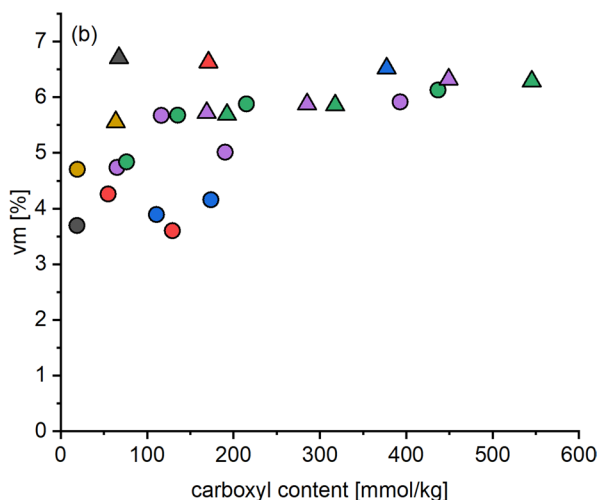
Values of the parameters  $k$  and  $C$  are shown in Fig. S5. Neither parameter changed significantly with the degree of carboxymethylation, either in the protonated and deprotonated forms of the fibers. The values for the deprotonated forms were only marginally greater than for the protonated forms. Whereas the values of  $C$  did not change significantly between fiber types or treatment conditions; the values of  $k$  were marginally greater for CV as compared to Co and for fibers from treatment in 4.0 M NaOH as compared to 0.5 M NaOH.

### Moisture sorption kinetics

The moisture sorption rates of cellulosic materials are frequently derived from the “Parallel Exponential Kinetics” (PEK) model (Kohler et al. 2003), depicted in Eq. 5.

$$M_t = M_{\infty 1} \left( 1 - e^{-\left(\frac{t}{\tau_1}\right)} \right) + M_{\infty 2} \left( 1 - e^{-\left(\frac{t}{\tau_2}\right)} \right) \quad (5)$$

where,  $M_t$  = moisture regain (%) at time ‘ $t$ ’ (min)  $M_{\infty 1}$ ,  $M_{\infty 2}$  = moisture regain equilibria attained through



fibers treated only in 4.0 mol/L NaOH (yellow circle, yellow triangle), in 0.5 mol/L NaOH at 30 °C (red circle, red triangle), in 0.5 mol/L NaOH at 50 °C (blue circle, blue triangle), in 4.0 mol/L NaOH at 30 °C (green circle, green triangle) and in 4.0 mol/L NaOH at 50 °C (violet circle, violet triangle)

each of the two independent processes,  $\tau_1$ ,  $\tau_2$  = characteristic times (min) to reach  $0.6321 M_\infty$  in the individual processes.

In the model, the total moisture sorption is envisaged to be the sum of two first-order processes that occur in parallel but are independent of each other. One of the processes is labeled “slow” and the other “fast”, and each has their individual contribution, which sum up to the total moisture regain at equilibrium. The model is intended as a ‘pragmatic, numerical’ approach to highlight differences between materials, without attempting to characterize any of the underlying sorbate-adsorbent interaction mechanisms. Nevertheless, use of the PEK model is robustly criticized for being inadequate, principally on grounds that the derived parameters are not representative of any physical phenomena or of structural elements in cellulose (Thybring et al. 2019).

For that reason, in this work, the PEK model was employed to derive “ $t_{50}$ ”, defined as the time (in minutes) required for sorption of half the equilibrium moisture regain. A direct determination from experimental data was not feasible, since each sample was measured only once per 10 min, and that would not allow for a good resolution in the results. Hence, the experimental data were first modeled with Eq. 5 (standard error of fits ranged between 0.007–0.062), and the  $t_{50}$  were derived from the obtained model. To normalize for differences in sorption levels, the  $t_{50}$  divided by the equilibrium moisture regain (i.e.,  $t_{50}/MR_{eq}$ ) was employed to highlight differences in the rate of sorption between experimental substrates. Higher values indicate lower rates of sorption. See Fig. S6 and S7 for results from the protonated and deprotonated forms of the fibers respectively.

There were generally no differences of  $t_{50}/MR_{eq}$  between the deprotonated and protonated sets except in the humidity interval of 0–10%, where the deprotonated fibers exhibited slower sorption rates. In both sets, the  $t_{50}/MR_{eq}$  increased gradually with rise in degree of carboxymethylation in the humidity interval of 0–60% (see parts a–f in Fig. S6 and S7), but at higher humidity levels, there appeared no influence of degree of carboxymethylation on the sorption rate (see parts g–i in Fig. S6 and S7). No differences could be discerned between fiber types or of the alkali level in treatment, except among protonated fibers in the humidity interval of 30–60%, where the sorption rate

of CV fibers was generally slower than that of the Co (see parts d–f in Fig. S6).

## Discussion

Cellulose interactions with water increase with rising charge density, and the extents are proportional to the polarity of polymer functional groups as well as the electric field intensities of counter ions. Carboxyl groups are more polar than hydroxyls and thus carboxymethylation promotes greater interactions with water; the electric field intensity of sodium ions is greater than that of hydrogen and thus water interactions with the sodium salt of carboxyl groups (i.e., their deprotonated form) is greater than with their protonated form (Berthold et al. 1994, 1996; Hubbe and Rojas 2008; Zhang et al. 2018). These trends were observed also in the results of this work. Both water retention and water vapor (i.e., moisture) sorption generally increased with the degree of carboxymethylation; and for both parameters, the values for deprotonated forms of fibers were greater than that of the corresponding protonated forms. The ratio of values, deprotonated-to-protonated, from measurements of both water retention and moisture sorption, were found to change only with degree of carboxymethylation with no influence from other variables (i.e., fiber type and NaOH level in treatment). Only in case of moisture sorption, the relative humidity was also observed to influence the ratios. Of interest are the differences observed as function of fiber type and of NaOH level in treatment, *at comparable degrees of carboxymethylation*. The changes in degree of polymerization on carboxymethylation, of on average *ca.* 10% and 15% in CV and Co respectively, are too low to have contributed significantly to the observed changes in water retention and moisture sorption.

The water retention, a measure of fiber swelling in water, increased in the order of fiber type /NaOH level  $Co/0.5\ M < Co/4.0\ M \cong CV/0.5\ M < CV/4.0\ M$ . The swelling level of carboxymethyl cellulose is inversely proportional to the degree of polymerization of the cellulose. The CV fibers exhibited a lower degree of polymerization than Co, which will contribute to the observed order. Treatments with 4.0 M NaOH is known to increase porosity and thereby also the water retention (Jaturapiree et al. 2008; Öztürk et al. 2009). Evidence of that was observed in this work, from the differences of water retention between

fibers that were only cleaned and those that were treated with 4.0 M NaOH alone. A further contribution is the depth to which the carboxymethylation occurs within fibers. It has been shown that the water retention is greater for cellulose carboxymethylated through the bulk as compared to when the substitution is limited to the surface alone (Torgnysdotter and Wågberg 2003; Hubbe and Rojas 2008). In previous work (Bogner et al. 2024a, b), we reported evidence of greater depths of carboxymethylation in CV as compared to Co and in fibers from treatment in 4.0 M NaOH as compared to 0.5 M NaOH, from FTIR spectroscopy and dye sorption measurements; and that appears reflected in the results of water retention as well.

The change in moisture regain equilibria with rise in degree of carboxymethylation was lower in CV as compared to Co. The baseline of moisture sorption in CV fibers, i.e., in the reference fibers, was significantly greater than that in Co, which may be attributed to the greater levels of accessibility in CV as compared to Co (Bredereck and Hermanutz 2005). Thus, it appears the carboxymethylation resulted in smaller improvements of moisture sorption in the CV relative to the initially high moisture regain. A further difference was that CV fibers from 0.5 M NaOH treatments exhibited greater moisture regain as compared to fibers from 4.0 M NaOH treatments, whereas the reverse was observed for the Co. The difference may be attributed to greater hornification in the viscose after the 4 M NaOH treatments. The fibers after carboxymethylation treatments were washed and dried. Drying causes irreversible losses of pore volume in cellulose (termed ‘hornification’), and the extents increase with the degree of swelling before the drying step (Klemm et al. 1998b; Jaturapiree et al. 2011). Swelling levels are higher in CV as compared to Co (You et al. 2021), and thus hornification levels in CV would also be higher.

The differences described above in moisture regain equilibria were also reflected in the GAB model parameter of  $v_m$ , whereas no significant differences were observed in the parameters  $k$  and  $C$ . For polysaccharides in general, caution is recommended in the attribution of physical significance to GAB model parameters, as the parameter estimates do not match results of other independent measurements of the same phenomena (Timmermann 2003; Thybring et al. 2021). Thus,  $v_m$  may be regarded as a measure

of accessibility in general, but not specifically of moisture sorbed in a monomolecular layer. The  $C$  and  $k$  are to be understood as indicators of profile shape of the type II isotherm, the former of the knee in the lower range of humidity (at *ca.* 30% relative humidity) and the latter of upswing in the higher range of humidity (at *ca.* 70% relative humidity). Thus, the GAB model parameter estimates indicate that the accessibility among the different samples increased in the order of fiber type/NaOH level: Co/0.5 M < Co/4.0 M ≤ CV/4.0 M < CV 0.5 M, and that there were no significant differences in the shapes of the isotherm profiles.

The moisture sorption rates were found to become slower with rise in the degree of carboxymethylation (the  $t_{50}/MR_{eq}$  increased gradually), but such effects were evident only until relative humidity of 60%. The sorption at higher humidity levels is dominated by capillary condensation, as indicated by the upward swing in sorption equilibria beginning at *ca.* 70% relative humidity, and here there was no influence of carboxymethylation level on sorption rates. Beyond isolated effects, the fiber type or alkali level in treatment were not observed to influence the moisture sorption rates.

No significant differences of hysteresis in the moisture sorption–desorption cycle were observed between any of the samples. Hysteresis is related to water-induced ‘plasticization’ or softening of the polymer (Hou et al. 2022), and it appears that the carboxymethylation, in the range of values obtained in this work, did not influence that aspect of fiber properties.

## Conclusion

A greater impact of fiber carboxymethylation was observed on their interactions with liquid water (i.e., water retention) as compared to water vapor (i.e., moisture sorption), as the differences in water retention between the carboxymethylated and reference fibers were greater than that of moisture sorption. In addition to the degree of carboxymethylation, the underlying structure also influenced the response of fibers to liquid water and to moisture, in terms of accessibility, swellability (which is related to the degree of polymerization) and hornification levels. No effect of the distribution of substituted

carboxymethyl groups through fiber structures could be detected on moisture sorption levels, but there was evidence of it in their water retention values. Interestingly, whereas a greater depth of carboxymethylation promoted higher water retention (as observed in this work), it was observed to militate against carboxyl group accessibility to dye molecules (observed in previous work). Thus, a greater depth of carboxymethylation would be detrimental or conducive to performance depending on the metric: dye sorption or water retention, respectively. It highlights the contrasting effects that may arise, of a given set of treatment parameters (fiber type, alkali level in treatment), on efficacy of the product performance.

Comparisons between the fiber types of the level of carboxymethylation at the core regions, and assessments of the impact of pore distribution in fibers on the distribution of substituted carboxymethyl groups are works in progress. Of interest will also be to determine if the carboxymethylation changed fiber mechanical properties and if there was any fibrillation of the fibers. Further questions of interest include: the behavior of fibers in measurements of metal complexation, the effect of using a different alkali in treatments (e.g., KOH), and differences between the fiber types in other modification reactions (e.g., acetylation).

**Author contributions** Paul Bogner: investigation, methodology, visualization, writing—original draft; Inge Schlapp-Hackl: investigation, writing—review & editing, Michael Hummel: investigation, writing—review & editing, Thomas Bechtold: conceptualization, supervision, writing—review & editing; Tung Pham: conceptualization, supervision, writing—review & editing, funding acquisition; Avinash P. Manian: conceptualization, supervision, writing—review & editing.

**Funding** Open access funding provided by University of Innsbruck and Medical University of Innsbruck. The research leading to these results was performed in the frame of the project “Textile Competence Center Vorarlberg 2 (Project No. 882502)” funded under the COMET program – Competence Centers for Excellent Technologies – by the Federal Ministry for Climate Protection, Environment, Energy, Mobility, Innovation and Technology (BMK) and the Federal Ministry for Digitization and Business Location (BMDW), with co-financing from the federal province of Vorarlberg. The COMET program is administered by the Austrian Research Promotion Agency (FFG).

**Data availability** All data that support the findings of this study are available from the corresponding author, APM, upon reasonable request.

#### Declarations

**Conflict of interest** The authors declare no competing interests.

**Ethical approval** Not applicable, because this article does not contain any studies with human or animal subjects.

**Open Access** This article is licensed under a Creative Commons Attribution 4.0 International License, which permits use, sharing, adaptation, distribution and reproduction in any medium or format, as long as you give appropriate credit to the original author(s) and the source, provide a link to the Creative Commons licence, and indicate if changes were made. The images or other third party material in this article are included in the article’s Creative Commons licence, unless indicated otherwise in a credit line to the material. If material is not included in the article’s Creative Commons licence and your intended use is not permitted by statutory regulation or exceeds the permitted use, you will need to obtain permission directly from the copyright holder. To view a copy of this licence, visit <http://creativecommons.org/licenses/by/4.0/>.

#### References

- BeMiller JN (2019) Cellulose and cellulose-based hydrocolloids. Woodhead Publishing and AACC International Press, Duxford
- Berthold J, Desbrières J, Rinaudo M, Salmén L (1994) Types of adsorbed water in relation to the ionic groups and their counter-ions for some cellulose derivatives. *Polymer* 35:5729–5736. [https://doi.org/10.1016/S0032-3861\(05\)80048-5](https://doi.org/10.1016/S0032-3861(05)80048-5)
- Berthold J, Rinaudo M, Salmeri L (1996) Association of water to polar groups; estimations by an adsorption model for ligno-cellulosic materials. *Colloids Surf A Physicochem Eng Asp* 112:117–129. [https://doi.org/10.1016/0927-7757\(95\)03419-6](https://doi.org/10.1016/0927-7757(95)03419-6)
- Bogner P, Bechtold T, Pham T, Manian AP (2024a) Alkali induced changes in spatial distribution of functional groups in carboxymethylated cellulose. *Cellulose* 31:2833–2847. <https://doi.org/10.1007/s10570-024-05798-9>
- Bogner P, Mahmud-Ali A, Bechtold T, et al (2024b) Alkali induced changes in spatial distribution of functional groups in carboxymethylated cellulose—comparison

- of cotton and viscose fibers. *Cellulose* 31:7313–7324. <https://doi.org/10.1007/s10570-024-06036-y>
- Bredereck K, Hermanutz F (2005) Man-made cellulose. *Rev Prog Color Relat Top* 35:59–75. <https://doi.org/10.1111/j.1478-4408.2005.tb00160.x>
- Chen J, Wu J, Raffa P et al (2022) Superabsorbent Polymers: from long-established, microplastics generating systems, to sustainable, biodegradable and future proof alternatives. *Prog Polym Sci* 125:101475. <https://doi.org/10.1016/j.progpolymsci.2021.101475>
- Cleaver G (2015a) Analysis of Carboxymethyl Cellulose via GPC Viscometry. In: *Agil Technol Appl Note*. <https://www.agilent.com/cs/library/applications/5991-5827EN.pdf>
- Cleaver G (2015b) SEC Analysis of Carboxymethyl Cellulose. In: *Agil Technol Appl Note*. <https://www.agilent.com/cs/library/applications/5991-5792EN.pdf>
- Eremeeva TE, Bykova TO (1998) SEC of mono-carboxymethyl cellulose (CMC) in a wide range of pH; Mark-Houwink constants. *Carbohydr Polym* 36:319–326. [https://doi.org/10.1016/S0144-8617\(97\)00259-2](https://doi.org/10.1016/S0144-8617(97)00259-2)
- Gu H, He J, Huang Y, Guo Z (2012) Water soluble carboxymethylcellulose fibers derived from alkalization-etherification of viscose fibers. *Fibers Polym* 13:748–753. <https://doi.org/10.1007/s12221-012-0748-x>
- Heinze T, El Seoud OA, Koschella A (2018) Etherification of cellulose. In: Heinze T, El Seoud OA, Koschella A (eds) *Cellulose derivatives: synthesis, structure, and properties*. Springer International Publishing, Cham, pp 429–477
- Hou S, Wang J, Yin F et al (2022) Moisture sorption isotherms and hysteresis of cellulose, hemicelluloses and lignin isolated from birch wood and their effects on wood hygroscopicity. *Wood Sci Technol* 56:1087–1102. <https://doi.org/10.1007/s00226-022-01393-y>
- Hubbe MA, Rojas OJ (2008) Colloidal stability and aggregation of lignocellulosic materials in aqueous suspension: a review. *BioResources* 3:1403–1418. <https://doi.org/10.15376/biores.3.4.1419-1491>
- Ibrahim NA, Eid BM, Abd El-Ghany NA, Mabrouk EM (2020) Polyfunctional cotton cellulose fabric using proper biopolymers and active ingredients. *J Text Inst* 111:381–393. <https://doi.org/10.1080/00405000.2019.1634459>
- Iwata N (2021) Analysis of carboxymethyl cellulose using an integrated HPLC system. In: *Shimadzu Appl News*. [https://www.shimadzu.com/an/sites/shimadzu.com.an/files/pim/pim\\_document\\_file/applications/application\\_note/14238/an\\_01-00207-en.pdf](https://www.shimadzu.com/an/sites/shimadzu.com.an/files/pim/pim_document_file/applications/application_note/14238/an_01-00207-en.pdf)
- Jaturapiree A, Ehrhardt A, Groner S et al (2008) Treatment in swelling solutions modifying cellulose fiber reactivity—part I: accessibility and sorption. *Macromol Symp* 262:39–49. <https://doi.org/10.1002/masy.200850205>
- Jaturapiree A, Manian AP, Lenninger M, Bechtold T (2011) The influence of alkali pretreatments in lyocell resin finishing—Changes in fiber accessibility to crosslinker and catalyst. *Carbohydr Polym* 86:612–620. <https://doi.org/10.1016/j.carbpol.2011.04.085>
- Klemm D, Philipp B, Heinze T, et al (1998a) General Considerations on Structure and Reactivity of Cellulose: Section 2.2–2.2.3. In: *Comprehensive cellulose chemistry*. John Wiley & Sons, Ltd, Weinheim, Germany, pp 43–82. <https://doi.org/10.1002/3527601929.CH2C>
- Klemm D, Philipp B, Heinze T, et al (1998b) General considerations on structure and reactivity of cellulose: Section 2.1–2.1.4. In: *Comprehensive cellulose chemistry*. John Wiley & Sons, Ltd, Weinheim, Germany, pp 9–29. <https://doi.org/10.1002/3527601929.ch2a>
- Kohler R, Dück R, Ausperger B, Alex R (2003) A numeric model for the kinetics of water vapor sorption on cellulose reinforcement fibers. *Compos Interfaces* 10:255–276. <https://doi.org/10.1163/156855403765826900>
- Kunjalukkal Padmanabhan S, Lamanna L, Friuli M et al (2023) Carboxymethylcellulose-based hydrogel obtained from bacterial cellulose. *Molecules* 28:829. <https://doi.org/10.3390/molecules28020829>
- Li Z-W, Du Z-M, Wang Y-W et al (2022) Chemical modification, characterization, and activity changes of land plant polysaccharides: a review. *Polymers (Basel)* 14:4161. <https://doi.org/10.3390/polym14194161>
- Liao Y, Alam N, Fatehi P (2022) Semitransparent films from low-substituted carboxymethylated cellulose fibers. *J Mater Sci* 57:10407–10424. <https://doi.org/10.1007/s10853-022-07262-0>
- Liu Y, Wei Y, He Y et al (2023) Large-Scale preparation of carboxylated cellulose nanocrystals and their application for stabilizing pickering emulsions. *ACS Omega* 8:15114–15123. <https://doi.org/10.1021/acsomega.2c08239>
- Manian AP, Braun DE, Široká B, Bechtold T (2022) Distinguishing liquid ammonia from sodium hydroxide mercerization in cotton textiles. *Cellulose* 29:4183–4202. <https://doi.org/10.1007/s10570-022-04532-7>
- Mischnick P, Momcilovic D (2010) Chemical structure analysis of starch and cellulose derivatives. *Adv Carbohydr Chem Biochem* 64:117–210. [https://doi.org/10.1016/S0065-2318\(10\)64004-8](https://doi.org/10.1016/S0065-2318(10)64004-8)
- Miyamoto H, Sakakibara K, Wataoka I et al (2018) Interaction of water molecules with carboxyalkyl cellulose. In: Rosenau T, Potthast A, Hell J (eds) *Cellulose science and technology*. John Wiley & Sons Ltd, Hoboken, pp 127–141
- Nada A-AMA, Kamel S, El-Sakhawy M (2000) Thermal behaviour and infrared spectroscopy of cellulose carbamates. *Polym Degrad Stab* 70:347–355
- Nelson ML, O'Connor RT (1964) Relation of certain infrared bands to cellulose crystallinity and crystal lattice type. Part II: a new infrared ratio for estimation of crystallinity in celluloses I and II. *J Appl Polym Sci* 8:1325–1341. <https://doi.org/10.1002/app.1964.070080323>
- O'Connor RT, Dupré EF, Mitcham D (1958) Applications of infrared absorption spectroscopy to investigations of cotton and modified cottons: part I. Physical and crystalline modifications and oxidation. *Text Res J* 28:382–392. <https://doi.org/10.1177/004051755802800503>
- O'Sullivan AC (1997) Cellulose: the structure slowly unravels. *Cellulose* 4:173–207. <https://doi.org/10.1023/a:1018431705579>
- Oh SY, Il YD, Shin Y et al (2005a) Crystalline structure analysis of cellulose treated with sodium hydroxide and carbon dioxide by means of X-ray diffraction and FTIR spectroscopy. *Carbohydr Res* 340:2376–2391. <https://doi.org/10.1016/j.carres.2005.08.007>
- Oh SY, Il YD, Shin Y, Seo G (2005b) FTIR analysis of cellulose treated with sodium hydroxide and carbon dioxide.

- Carbohydr Res 340:417–428. <https://doi.org/10.1016/j.carres.2004.11.027>
- Öztürk HB, Potthast A, Rosenau T et al (2009) Changes in the intra- and inter-fibrillar structure of lyocell (TENCEL®) fibers caused by NaOH treatment. *Cellulose* 16:37–52. <https://doi.org/10.1007/s10570-008-9249-x>
- Pitkänen L, Sixta H (2020) Size-exclusion chromatography of cellulose: observations on the low-molar-mass fraction. *Cellulose* 27:9217–9225. <https://doi.org/10.1007/S10570-020-03419-9/TABLES/2>
- Potthast A, Rosenau T, Buchner R et al (2002) The cellulose solvent system N, N-dimethylacetamide/lithium chloride revisited: the effect of water on physicochemical properties and chemical stability. *Cellulose* 9:41–53. <https://doi.org/10.1023/A:1015811712657>
- Rác I, Deák A, Borsa J (1995) Fibrous carboxymethylcellulose by pad roll technology. *Text Res J* 65:348–354. <https://doi.org/10.1177/004051759506500607>
- Rissanen M, Schlapp-Hackl I, Sawada D et al (2023) Chemical recycling of hemp waste textiles via the ionic liquid based dry-jet-wet spinning technology. *Text Res J* 93:2545–2557. [https://doi.org/10.1177/00405175221143744/ASSET/IMAGES/LARGE/10.1177\\_00405175221143744-FIG5.JPEG](https://doi.org/10.1177/00405175221143744/ASSET/IMAGES/LARGE/10.1177_00405175221143744-FIG5.JPEG)
- Röder T, Potthast A, Rosenau T et al (2002) The effect of water on cellulose solutions in DMAc/LiCl. *Macromol Symp* 190:151–160. <https://doi.org/10.1002/masy.200290011>
- Thakur D, Seo S, Hyun J (2023) Three-dimensional triboelectric nanogenerator with carboxymethylated cellulose nanofiber and perfluoroalkoxy films. *J Ind Eng Chem* 123:220–229. <https://doi.org/10.1016/j.jiec.2023.03.037>
- Thommes M, Kaneko K, Neimark AV et al (2015) Physisorption of gases, with special reference to the evaluation of surface area and pore size distribution (IUPAC technical report). *Pure Appl Chem* 87:1051–1069. <https://doi.org/10.1515/pac-2014-1117>
- Thybring EE, Boardman CR, Glass SV, Zelinka SL (2019) The parallel exponential kinetics model is unfit to characterize moisture sorption kinetics in cellulosic materials. *Cellulose* 26:723–735. <https://doi.org/10.1007/s10570-018-2134-3>
- Thybring EE, Boardman CR, Zelinka SL, Glass SV (2021) Common sorption isotherm models are not physically valid for water in wood. *Colloids Surf A Physicochem Eng Asp* 627:127214. <https://doi.org/10.1016/j.colsurfa.2021.127214>
- Timmermann EO (2003) Multilayer sorption parameters: BET or GAB values? *Colloids Surf A Physicochem Eng Asp* 220:235–260. [https://doi.org/10.1016/S0927-7757\(03\)00059-1](https://doi.org/10.1016/S0927-7757(03)00059-1)
- Torgnysdotter A, Wågberg L (2003) Study of the joint strength between regenerated cellulose fibres and its influence on the sheet strength. *Nord Pulp Pap Res J* 18:455–459. <https://doi.org/10.3183/npprj-2003-18-04-p455-459>
- Wach RA, Mitomo H, Nagasawa N, Yoshii F (2003) Radiation crosslinking of carboxymethylcellulose of various degree of substitution at high concentration in aqueous solutions of natural pH. *Radiat Phys Chem* 68:771–779. [https://doi.org/10.1016/S0969-806X\(03\)00403-1](https://doi.org/10.1016/S0969-806X(03)00403-1)
- Wang J, Liu M, Duan C et al (2019) Preparation and characterization of cellulose-based adsorbent and its application in heavy metal ions removal. *Carbohydr Polym* 206:837–843. <https://doi.org/10.1016/j.carbpol.2018.11.059>
- Wang Z, Jiang Y, Mao L et al (2023) Pilot-scale preparation of cellulose/carboxymethylcellulose composite fiber for methylene blue adsorption. *Cellulose* 30:3611–3623. <https://doi.org/10.1007/s10570-023-05109-8>
- Yan H, Zhang W, Kan X et al (2011) Sorption of methylene blue by carboxymethyl cellulose and reuse process in a secondary sorption. *Colloids Surf A Physicochem Eng Asp* 380:143–151. <https://doi.org/10.1016/j.colsurfa.2011.02.045>
- You X, Chen F, Ma Y et al (2021) Single fiber swelling behavior for natural and man-made cellulose fibers under alkaline treatment. *Cellulose* 28:11287–11298. <https://doi.org/10.1007/s10570-021-04280-0>
- Zhang H, Hou Y, Yu P et al (2018) Deconstruction and dissolving of a fibrous sodium carboxymethyl cellulose network in a water solution. *BioResources* 13:8132–8142. <https://doi.org/10.15376/biores.13.4.8132-8142>

**Publisher's Note** Springer Nature remains neutral with regard to jurisdictional claims in published maps and institutional affiliations.